# Pivoting a Large Object: Whole-body Manipulation by a Humanoid Robot


Eiichi Yoshida[1], Pierre Blazevic[2], Vincent Hugel[2], Kazuhito Yokoi[1] and Kensuke Harada[3]

[1]*AIST/ISRI-CNRS/STIC Joint French-Japanese Robotics Laboratory (JRL)*
*AIST Central 2, Umezono 1-1-1, Tsukuba, Ibaraki 305-8568 Japan*
*{ e.yoshida, kazuhito.yokoi}@aist.go.jp*

[2]*LRV - Laboratoire de Robotique de Versailles*
*10/12 avenue de l'Europe, 78140 Vélizy, France*
*{ blazevic, hugel } @lrv.uvsq.fr*

[3]*Humanoid Research Group, Intelligent Systems Research Institute,*
*National Institute of Advanced Industrial Science and Technology (AIST)*
*AIST Central 2, Umezono 1-1-1, Tsukuba, Ibaraki 305-8568 Japan*
*kensuke.harada@aist.go.jp*


April 28, 2006


**Abstract**

In this paper we present a method of whole-body manipulation of large objects by a humanoid robot using a pivoting motion. Pivoting manipulation can be an alternative to pushing or lifting for more dexterous and stable operation, which is often used by humans to move large and bulky furniture. This paper describes a method and control techniques for a humanoid robot to perform the manipulation of a large object through whole-body motion by applying this pivoting motion. For this purpose, first the object is manipulated by two arms of a humanoid robot using impedance control for grasping, together with body balancing control while the robot stays at the same place. Next, the movement of the humanoid robot itself is performed by stepping with the help of resolved momentum control (RMC) to guarantee the robot stability. The proposed manipulation method is validated through dynamic simulation and real

hardware experiment of the humanoid robot HRP-2 performing the pivoting task.

# 1 Introduction

Research on humanoid robots has lead to prototypes that can perform complicated tasks, such as manipulation, navigation in dynamic environments, or serving tasks.

The manipulation task is one of promising application areas for humanoid robots since they have a high potential ability of executing of a variety of tasks by fully exploiting their high mobility and adaptability coming from its large number of degrees of freedom. Especially, manipulating bulky objects through a whole-body motion is suitable for them, which has been difficult for other types of robots. This paper focuses on the manipulation by a humanoid robot of large objects by introducing pivoting motions [1]. This manipulation method has several advantages such as dexterity and stability over other methods like pushing or lifting. Furthermore, the concept of a humanoid manipulating an object in contact with the ground poses interesting research challenges. The dynamic balance of the robot cannot be managed in the same way as in the case of the robot simply walking. The manipulated object brings a new kinematic chain and exerts a reaction force on the robot that must be taken into account. To cope with those problems, position and impedance control framework is first introduced to grasp and manipulate the object, together with a whole-body balancing control. Then resolved momentum control (RMC) [2] is adopted to allow the robot to step forward after manipulation by keeping the hand position with the object.

This paper is organized as follows. The next section presents the related work on the subject of manipulation tasks. Section 3 proposes an algorithm to deal with the manipulation, followed by the description of control techniques included in the algorithm in Section 4. Section 5 gives simulation results using the dynamic simulator OpenHRP, whose results are verified by hardware experiments using HRP-2 humanoid platform described in section 6 before concluding the paper.

# 2 Related Work

For manipulation of large objects that cannot be lifted we can make use of "non-prehensile manipulation" methods such as pushing [3, 4] or tumbling [5]. Aiyama et al. proposed a graspless manipulation using pivoting motion [1], and also the analysis and planning have been reported by Maeda et al. [6].

On the other hand, whole-body manipulation tasks by humanoid robot have been investigated more and more intensively these years. The main manipulation methods developed so far are pushing [8, 9, 10] and lifting [11].

For a humanoid to manipulate a large object using a whole-body motion, pivoting manipulation (Fig. 1), which we humans also often employ for example to move an oil drum or a barrel, is considered to have advantages in the following aspects:

- **Precise positioning**: Since the object is not held in pushing, uncertainty is more significant than pivoting and tumbling has also limitation in reachability.

  Although some of those shortcomings can be overcome using sophisticated control methods [4, 5], the robot can move the object to the desired position in a more straightforward manner.

- **Adaptability to rough terrains**: Pushing is difficult to be used in rough terrains whereas pivoting can be easily adapted. Lifting and tumbling can be used, but pivoting is more advantageous in terms of flexibility of manipulation and variety in shape and weight of manipulated objects.

- **Stability**: Pivoting has advantage of lower risk of falling over lifting when manipulating large or heavy objects. Moreover, the manipulated object can help widening stability margin in some cases.

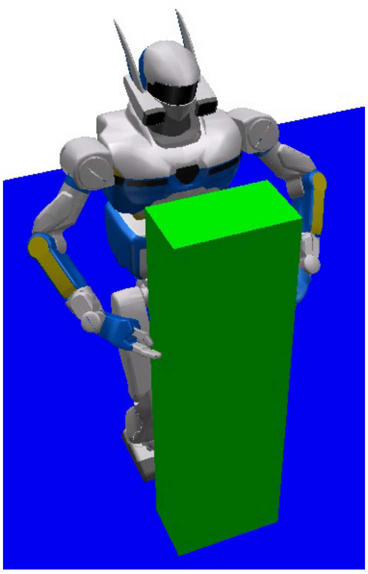

Figure 1: A humanoid robot grasping a box object

Table 1: Comparison of methods of manipulation of a large object by a humanoid

| | Precise positioning | Adaptability | Stability |
|---|---|---|---|
| Pushing | × | × | ○ |
| Lifting | ○ | △ | × |
| Tumbling | △ | △ | ○ |
| Pivoting | ○ | ○ | ○ |

○ : Suitable, △ : Can be used × : Not suitable

This comparison is summarized in Table 1. However, pivoting manipulation has not fully been exploited for humanoid robots due to the difficulty in coordinating manipulating motion with body balancing at whole-body level.

We therefore aim to establish a control method for pivoting manipulation by a whole-body motion of humanoid robot. The contribution of this paper is two-fold. The first point is the realization of pivoting manipulation that has not been implemented using humanoid platform so far, which provides new potential application fields that need dexterous manipulation by humanoid robots. The second contribution is the integration of such control techniques as impedance control for contact force, body balancing during manipulation and RMC for stepping motion, for the purpose of whole-body manipulation. In the following sections, pivoting manipulation by a humanoid robot is presented based on those techniques.

# 3 Pivoting Manipulation Algorithm

The manipulation is executed by repeating the following two phases:

- **Manipulation control phase**: The manipulation is done in a quasi-static way by repeating rotation of the object about an axis. The contact force to hold the object is controlled using impedance control.

  The manipulation is performed through whole-body motion coordination to achieve both manipulation and stable body balancing.

- **Robot motion phase**: The robot moves towards the object with the hands at the same position to continue manipulation. The body motion is planned through resolved momentum control (RMC).

Figure 2 summarizes the algorithm of the pivoting manipulation task. The detailed manipulation sequence is illustrated in Fig. 3 where the dotted and solid lines in each figure denote the states before and after the manipulation respectively.

1. The object is inclined by angle $\alpha$ around an axis $\boldsymbol{a}$ that includes a vertex $v$ on the plane so that the object has a point contact with the plane at $v$ (Fig. 3a).
2. The object is rotated by angle $\beta$ around the vertical axis $\boldsymbol{z}$ on vertex $v$ to move to the desired direction (Fig. 3b). As a result, the axis $\boldsymbol{a}$ is rotated to $\boldsymbol{a}'$ on the plane.
3. The object is rotated by $-\alpha$ around the rotated axis $\boldsymbol{a}'$ until the front bottom edge of the object touches ground. The displacement of the object is defined as the distance between the projected points of its center of mass before and after the manipulation. (Fig. 3c).
   (a) If the displacement of the object exceeds a value $D$, the robot steps toward the desired direction.
   (b) Otherwise continue to step 1 or terminate the motion.

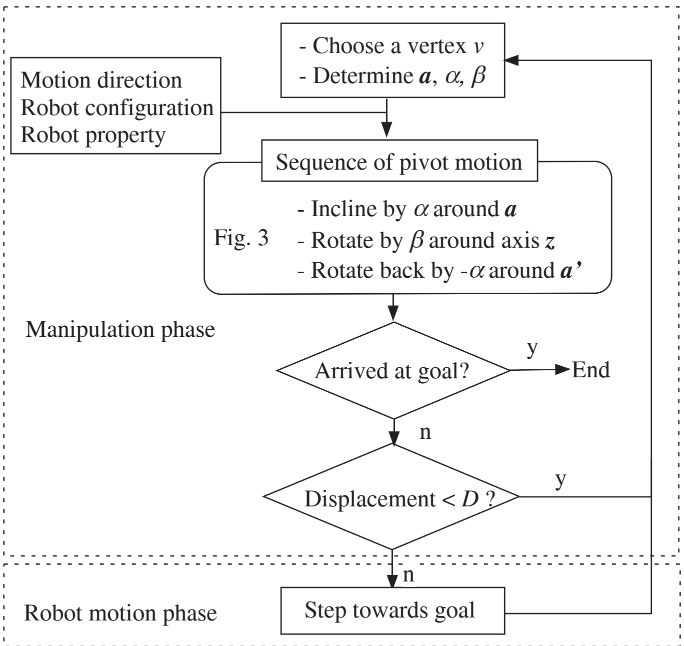


Figure 2: Flow of pivoting manipulation

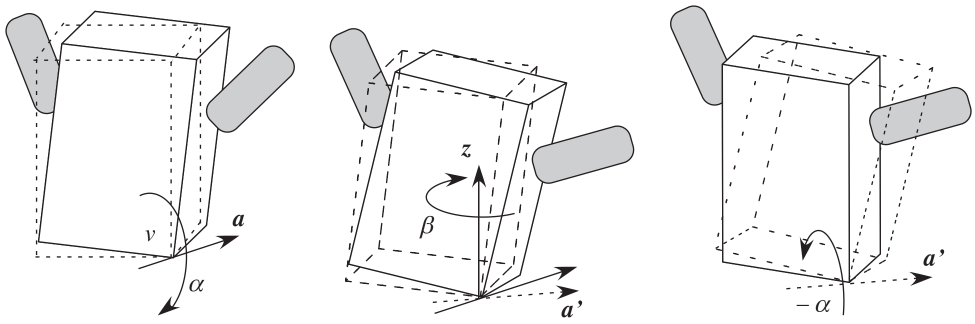


(a) Inclining (b) Rotating around z-axis (c) To initial contact

Figure 3: Sequence of pivot motion of a box object

The parameters $\alpha$, $\beta$ and $D$ must be designed so that the manipulated object follows the desired trajectory (Fig. 4). The working area and physical properties of the robot body must also be taken into account. The $\boldsymbol{a}$ axis and the vertex around which to incline the object are selected not to lose the stability of the robot and the object. In our case, the closer vertex to the robot is selected since smaller torque is required for the movement, and the direction of $\boldsymbol{a}$ is chosen so that the robot does not make a large forward motion.

The axis $\boldsymbol{z}$ is set to the vertical axis since no work is required for quasi-static motion around this axis. The angle $\beta$ depends on the constraint of robot motion capability as well as the desired trajectory of the robot. The hand trajectories can be calculated geometrically from the pivoting motion and contact points of the hand on the object.

To execute more complicated trajectory than that of Fig. 4, we will further need a planning strategy to determine those parameters, taking account of combination of stepping motion.

The next section details the manipulation control and robot motion for the pivoting task.

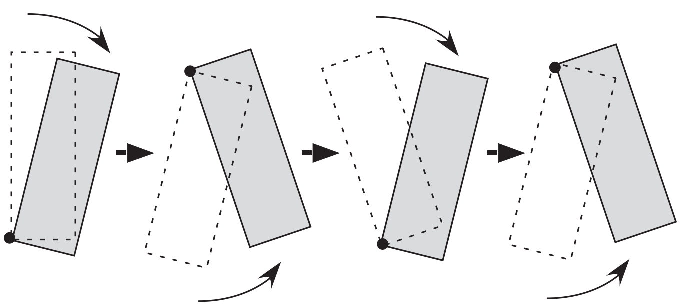

Figure 4: Object transporting by repeated pivoting

# 4 Control Techniques for Manipulation and Robot Motion

In this section we describe how the manipulation task is controlled by a humanoid robot. In the manipulation control phase, the robot is supposed to grasp the object by two hands firmly (Fig. 1) without slipping. First, we introduce impedance control to control the contact force to hold the object. Then, a method of body balancing is adopted to maintain the center of mass (CoM) in the supporting phase during manipulation. We assume that the manipulation is done for a rectangular box-shaped object in a quasi-static way by repeating the rotations on a plane as described in Fig. 3.

## 4.1 Grasping

Since we assume quasi-static motion, we adopt position control for robot hands to achieve the trajectory for the desired motion. For position-controlled robot as HRP-2 used for simulations and experiments, the output of the following impedance control is added to the position command of manipulation to regulate the contact force [9].

The robot hands are placed on the two sides of the object so that they can apply forces in the opposite direction. Let $x_H$ be the hand position which is controlled in the direction perpendicular to the object face, and let $f_x$ be the force exerted to the hand. The impedance control law to lead the force $f_x$ to the desired force $f_{xd}$ is given as

$$m\ddot{x}_H + c\dot{x}_H = f_{xd} - f_x. \tag{1}$$

where $m$ and $c$ are the mass and damper parameters. For grasping, one of the hands is controlled by this law and the other is controlled in position to avoid unnecessary oscillation. The control law is discretized in the simulation and experiment implementation.

## 4.2 Pivoting Manipulation

In our case, the robot holds the object rigidly by two hands as illustrated in Fig. 5. Let $\boldsymbol{p}_{pi}$ $(i = 1, 2)$ be the vector of position of each hand, $\boldsymbol{p}_g$ be the position of the center of gravity and $\boldsymbol{f}_{pi}$ be the force applied to each grasping point. The object is in static equilibrium when the following conditions are satisfied.

$$\boldsymbol{f}_o + \sum_{i=1}^{2} \boldsymbol{f}_{pi} + M\boldsymbol{g} = \boldsymbol{o}\,, \tag{2}$$

$$\sum_{i=1}^{2} \boldsymbol{p}_{pi} \times \boldsymbol{f}_{pi} + \boldsymbol{p}_g \times M\boldsymbol{g} = \boldsymbol{o}\,. \tag{3}$$

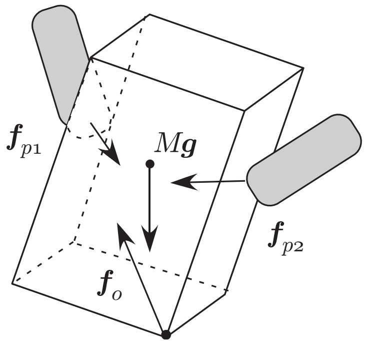


Figure 5: Forces for pivot motion

where $M\boldsymbol{g}$, $\boldsymbol{f}_o$ are the gravity vector and resistance force at the contact point respectively. In this research, we assume that the manipulation is executed quasi-statically and that no slipping occurs at the contact points. We also assume that the geometry and location of the object are known. The object is manipulated by moving each hand under the above condition. The contact forces are controlled by impedance control (1) by giving the desired contact force $f_{xd}$.

### 4.3 Whole-body Balancing

During the manipulation task, the robot should not only apply the necessary force to the hand for manipulation but also keep the balance of the whole body.

We adopt the method developed by Harada et al. [11]. The key idea is to control the waist position in order that the “static balancing point” is on the center of the foot supporting polygon. The static balancing point $\boldsymbol{p}_s = [x_s, y_s, 0]^T$ is the point on the floor to which all the resistance force from both hands and gravity are applied, which is equivalent to ZMP when no dynamics motion is generated. This is described as:

$$x_s - \bar{x} = -\sum_{i=1}^{2} \frac{z_{pi} f_{pi}{}^x + (x_{pi} - x_s) f_{pi}{}^z}{M_R\, g} \tag{4}$$

$$y_s - \bar{y} = -\sum_{i=1}^{2} \frac{z_{pi} f_{pi}{}^y + (y_{pi} - y_s) f_{pi}{}^z}{M_R\, g} \tag{5}$$

where $\boldsymbol{f}_{pi} = [f_{pi}{}^x, f_{pi}{}^y, f_{pi}{}^z]^T$ $(i = 1, 2)$, $\boldsymbol{p}_{pi} = [x_{pi}, y_{pi}, z_{pi}]^T$ and $\boldsymbol{g} = [0, 0, -g]$. The position of the CoM without external force is denoted by $\bar{\boldsymbol{p}} = [\bar{x}, \bar{y}, \bar{z}]^T$ here and $M_R$ is the total mass of the robot. Note that the sign in right-hand side of (4) and (5) is negative since the reaction force at each hand is $-\boldsymbol{f}_{pi}$.

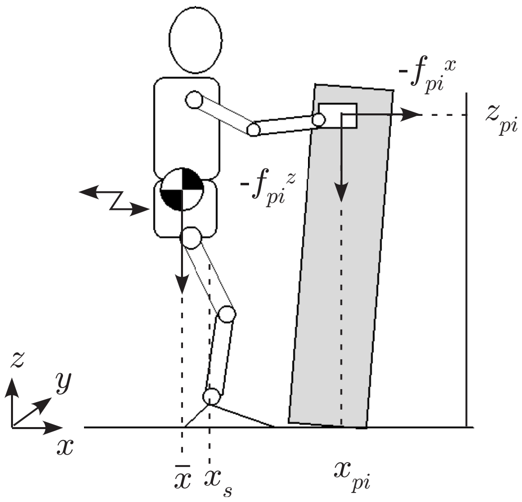


Figure 6: Body-balancing by moving waist position

The balancing control is performed by moving the position of the waist so that the position of the static balancing point $\boldsymbol{p}_s$ is at a desired position inside the convex hull of supporting area(s) (Fig. 6). The movement of the waist position can be approximated by the CoM position $\bar{\boldsymbol{p}}$ from the desired position $\boldsymbol{p}_d$ of $\boldsymbol{p}_s$ [11].

In this way, the force of pivoting manipulation is generated as a resulting compensation of disturbance due to the contact with the object.

## 4.4 Robot stepping motion

After a sequence of manipulation, the object will be displaced to a farther position from the robot. Now the robot itself needs to move in the desired direction of object transportation. It is, therefore, preferable that robot keep the hands on the object to easily go on the manipulation.

Here we introduce RMC that is a control framework where a humanoid robot is controlled such that the resulted total linear/angular momenta reach specified values [2]. It is well known that, for a humanoid robot to walk stably, the ZMP (Zero Moment Point) must be within the convex hull of the supporting area(s). By using RMC, we can control the CoM of the robot so that it is always within the convex hull of the supporting area(s) to maintain robot balance. Since the linear momentum $P$ depends on the time derivative of CoM position $r$ through the total mass $M_R$ as $P = M_R\dot{\boldsymbol{p}}_{\boldsymbol{g}}$, the position of CoM can be controlled by manipulating the linear momentum as $P = kM_R(\tilde{\boldsymbol{p}}_{\boldsymbol{g}} - \boldsymbol{p}_{\boldsymbol{g}})$, where the tilde denotes the reference value, and $k$ is the gain of the control scheme. Using this equation we are can calculate the desired linear momentum $P$ to control the robot CoM.

The hand position can be controlled based on an extended method of RMC developed by Neo et al. [12] by keeping the position of CoM inside the supporting area.

In this way, the robot can step towards the object with its both hands at the position keeping the contact, while the CoM is controlled always inside the convex hull of supporting area(s). Moreover, keeping the hand position on the object may help to maintain the equilibrium of the robot body.

# 5 Simulation

We have conducted a simulation of the proposed pivoting motion using the humanoid robot simulator OpenHRP [13] where the humanoid robot HRP-2 [14] is modeled. HRP-2 has 30 degrees of freedom with 1.54 [m] in height and 58 [kg] in weight. Wrists and ankles are equipped with force sensors. Since the input of force sensor is noisy, we use an average value of the last 20 samplings measured every 5 [ms]. The width, depth, and height of the object are 0.35[m], 0.2[m], and 1.2[m] respectively. The mass is 3[kg].

The parameters of the pivoting sequence are shown in Table 2. The directions of axes are given in Fig. 7(a). Here parameter $D$ is set to 50[mm] to prevent the arms from going into singular configuration and losing stability by extending arm too much. For the impedance control, we adopt $m$ = 10[kg], $c$ = 300[N·m$^{-1}$·s] and $f_{xd}$ = 25[N] respectively. The contact force $f_{xd}$ is determined for the robot to hold firmly to prevent the object from slipping because of gravity. The $z$ position of contact point is set to 0.62[m] and at the midpoint of the depth of the object in $x$ direction.

In the simulation, first the robot grasps the object firmly and stays at the original position until the contact force by impedance control stabilizes. The hand trajectories during the manipulation are computed geometrically by using the contact points of both hands and the motions described in Table 2. Position control is performed to follow the calculated hand trajectories and the impedance control law (1) is applied to one of the hands to maintain grasping during the manipulation.

Figure 7 shows the snapshots of the simulation. As can be seen, the humanoid robot successfully displaces the object by pivoting.

Table 2: Parameters of pivot motion

| Step | Type (in Fig. 3) | Axis* | Angle [deg] | Time [s] | Contact vertex ** | Description ** |
|---|---|---|---|---|---|---|
| 1 | (a) | $\boldsymbol{a}_1$ = (3, -1, 0) | $\alpha$ = 5.0 | 1.0 | NR | Inclining rightward |
| 2 | (b) | $\boldsymbol{z}$ = (0, 0, 1) | $\beta$ =-15.0 | 3.0 | NR | Rotating CW |
| 3 | (c) | $\boldsymbol{a}'_1$ = (3, -1, 0)*** | $\alpha$ = -5.0 | 1.0 | NR | Inclining back |
| 4 | (a) | $\boldsymbol{a}_2$ = (3, 1, 0) | $\alpha$ = -5.0 | 1.0 | NL | Inclining leftward |
| 5 | (b) | $\boldsymbol{z}$ = (0, 0, 1) | $\beta$ = 15.0 | 3.0 | NL | Rotating CCW |
| 6 | (c) | $\boldsymbol{a}'_2$ = (3, 1, 0)*** | $\alpha$ = 5.0 | 1.0 | NL | Inclining back |

* See Fig. 7 a for the reference frame. The angle between $\boldsymbol{x}$ and $\boldsymbol{a_1}$, $\boldsymbol{a_2}$ is 18.4 [deg] and -18.4[deg] respectively.

** NR: Near-Right, NL: Near-Left, CW: Clockwise, CCW: Counter-clockwise

*** Axis $\boldsymbol{a}'$ is rotated vector $\boldsymbol{a}$ around $\boldsymbol{z}$ by $\beta$.

We measure the displacement of the manipulated object, the contact forces, and center of the mass of the robot, to evaluate respectively the performance of the manipulation itself, impedance control, and the balance control.

Figure 8 shows the displacement of the center of mass of the manipulated object projected on the plane. Since the object is first inclined around the axis $\boldsymbol{a}$ before rotating around $\boldsymbol{z}$ axis, the $x$ displacement reduces first and then increases. This occurs twice and we can see the object is displaced by 0.073 [m] in $x$ direction.

Figure 9 shows the simulation results of the contact forces $f_{p1}$, $f_{p2}$ for both hands. As shown in the figure, the contact occurs at the very beginning when both hands are approaching the object. Then both the contact forces stabilize around the desired force $f_{xd}$ =25[N] at the beginning of the manipulation. The contact force decreased during the manipulation. It may be because the arms go to a stretched configuration

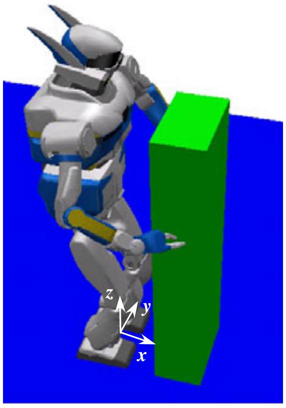


(a) Initial state

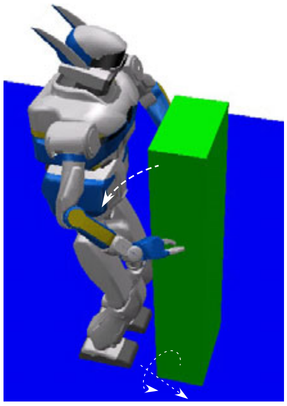

(b) Step 1: inclining rightward

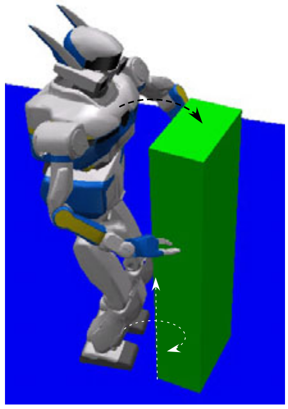

(c) Step 3: rotating CW

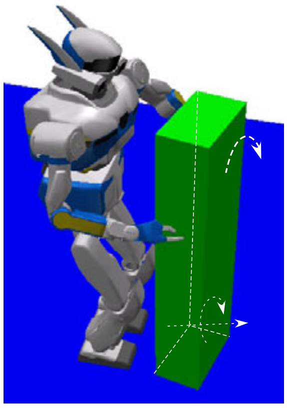

(d) Step 4: inclining leftward

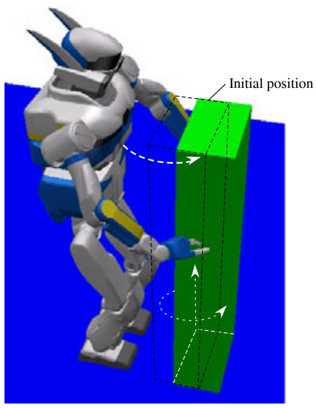


(e) Step 5: rotating CCW

Figure 7: Simulation results of pivoting motion

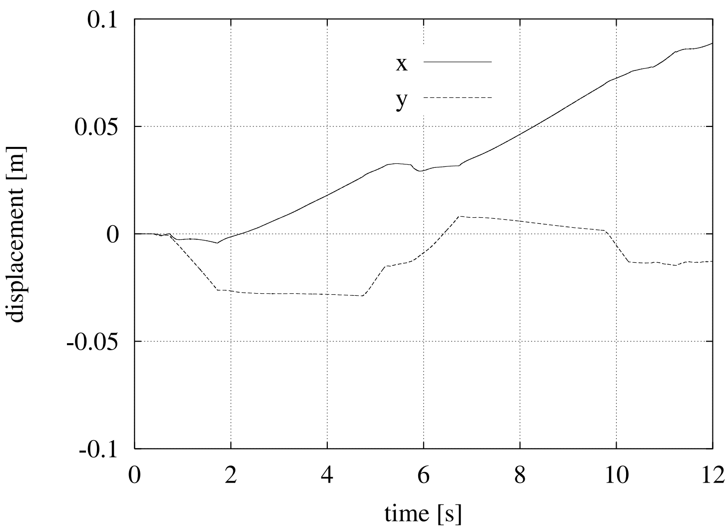


Figure 8: Displacement of the manipulated object

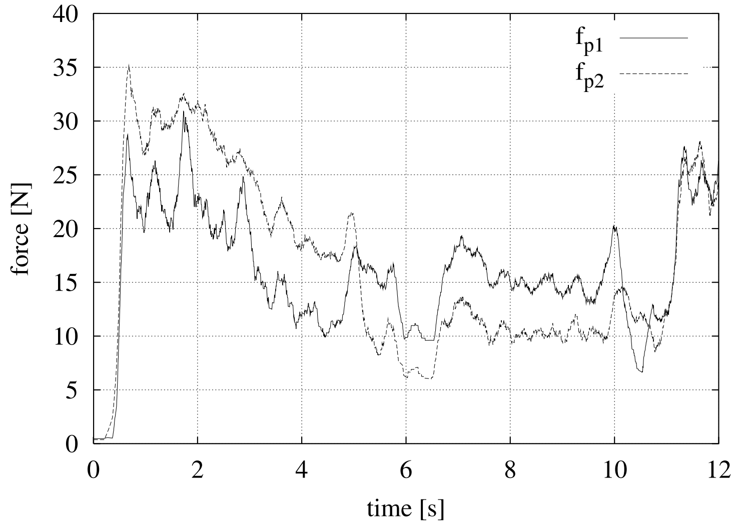


Figure 9: Contact forces of each hand

where it is difficult to generate the force in the desired direction during manipulation especially for the position controlled arm. However, the forces regain the desired value after the manipulation. This simulation result verifies that the usage of impedance control for contact force is sufficiently effective.

The $x$ coordinates of static balancing point $\boldsymbol{p_s}$ and CoM position $\bar{\boldsymbol{p}}$ without external force, $x_s$ and $\bar{x}$, are plotted in Fig. 10. Here $\bar{\boldsymbol{p}}$ represents an approximated movement of the waist position. Without balance controlling, $x_s$ would keep increasing as the robot reaches out the arms and force is applied to the hand during the manipulation until the robot falls down. In the graph, the static balancing point is regulated by

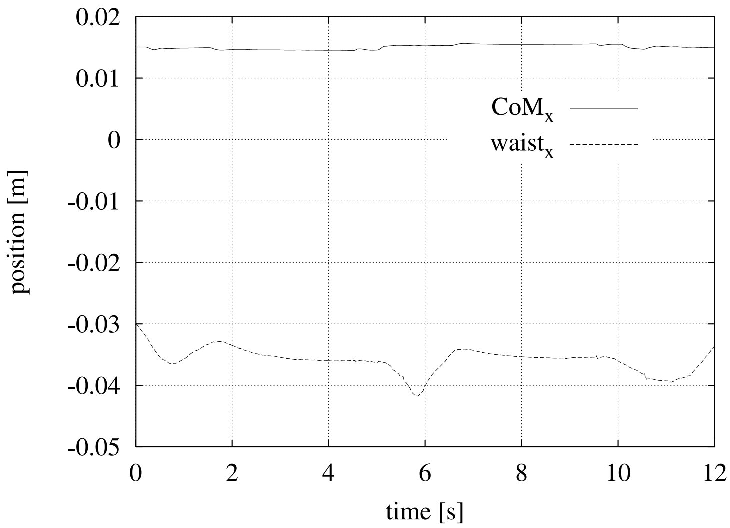


Figure 10: Center of mass and waist positions

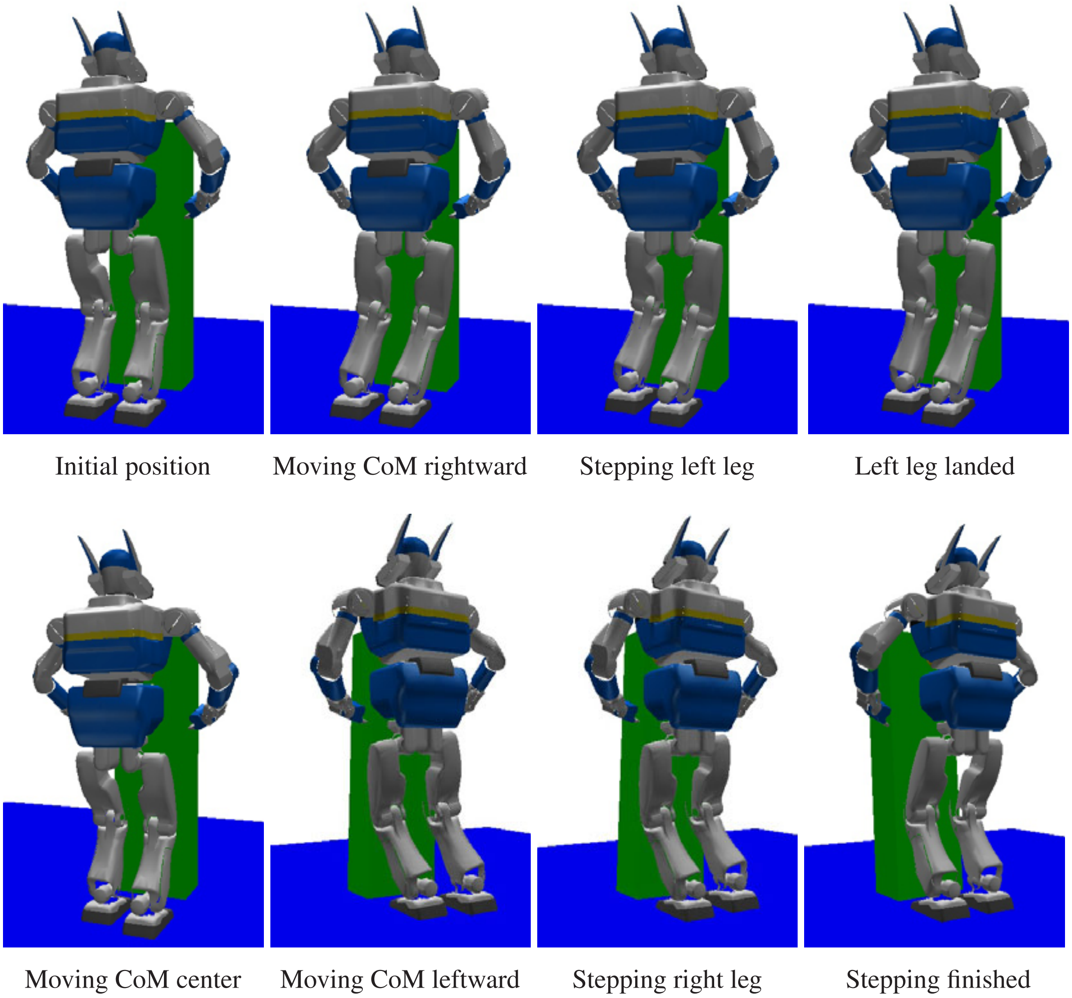


Figure 11: Stepping forward keeping the hands on the object

moving the waist position so that it coincides with the center of the feet (shift along x-axis of 0.015[m]) according to the balancing control.

The robot motion phase is simulated based on the proposed method. Figure 11 shows the sequence of stepping for forward motion. After the manipulation, the robot steps forward by 50[mm] by moving its feet alternatively, by keeping the hand on the object using RMC to maintain the whole body balance. As shown in Fig. 11, first robot moves its CoM on the right foot and then moves the left foot forward. The same sequence is repeated for the right foot. The simulation shows that robot can effectively moves towards the desired direction of manipulation.

# 6 Experimental Results

We have conducted an experiment of the manipulation control part in the same condition as in simulation using HRP-2 humanoid hardware platform. Thanks to the architecture of OpenHRP, the developed simulation software has binary compatibility with the robot hardware.

Figure 12 shows snapshots of the experiments using almost the same size and weight of the box as in simulation. As can be seen, the pivoting manipulation has been executed appropriately and the displacement in $x$ direction was around 0.06[m] as expected from simulation.

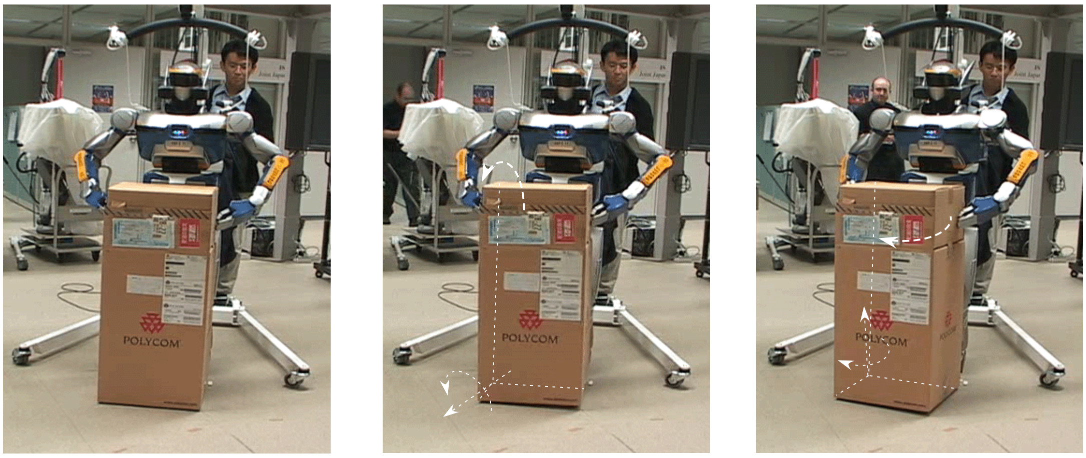


(a) Initial state (b) Step 1: inclining rightward (c) Step 3: rotating CW

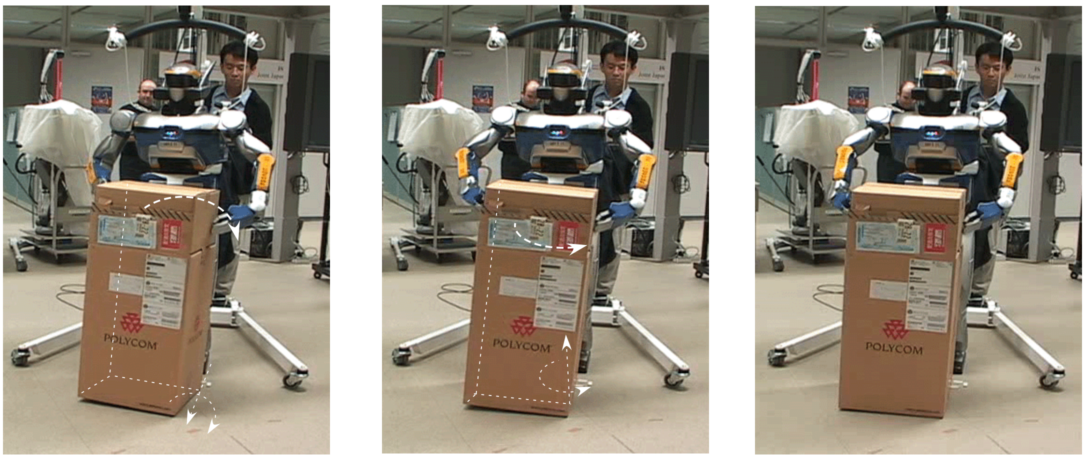


(d) Step 4: inclining leftward (e) Step 5: rotating CCW (f) Final state

Figure 12: Experiment of pivoting motion

Figure 13 shows the contact forces measured from wrist force sensors. Although the measured force shows similar characteristics with the simulation, one of the forces drops drastically at the end of manipulation. The manipulation experiment was successful; however, the arm configuration and grasping position need to be investigated for more reliable manipulation. The experimental result of the same values as the graph in Fig. 10 shows the effectiveness of balance control to keep the static balancing point in stable position as shown in Fig. 14.

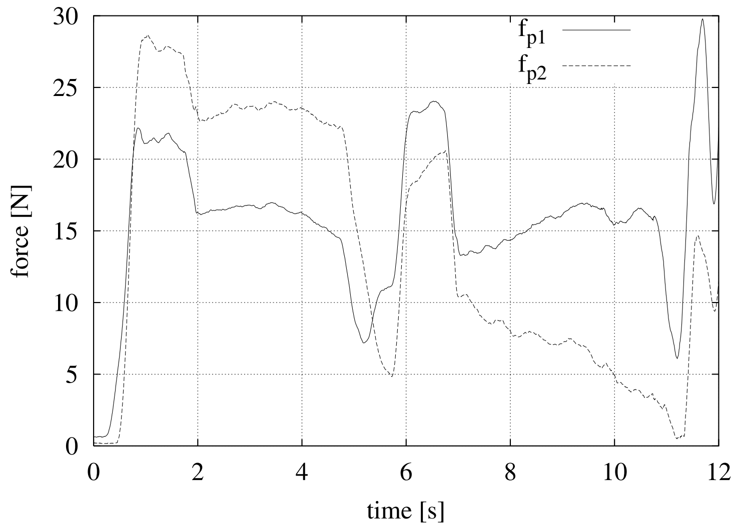


Figure 13: Experimental result of contact forces of each hand

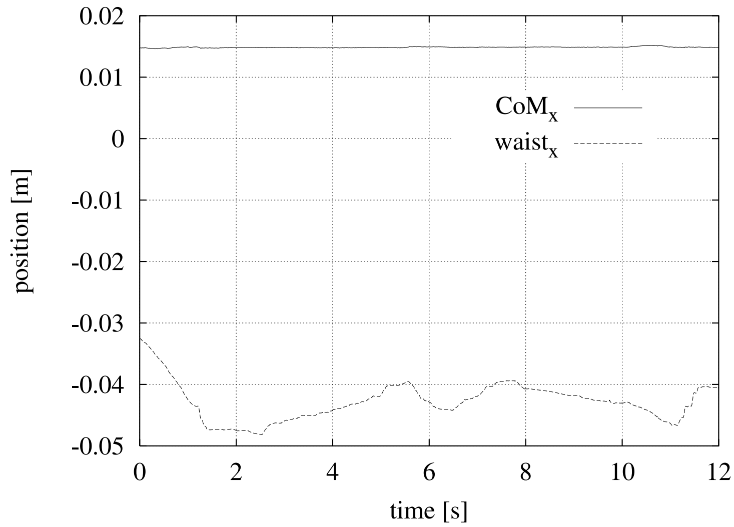


Figure 14: Experimental result of center of mass and waist positions

# 7 Conclusion

In this paper we have presented a pivoting manipulation as an application of a humanoid robot platform. By realizing this dexterous manipulation that enables precise displacement of heavy or bulky objects, the area to which humanoid robot are applied can be significantly extended.

We have proposed a sequence of pivoting motion composed of two phases, manipulation control and robot motion. In the former phase, impedance control and balancing control were introduced to control the required contact force for grasping and to maintain stability during manipulation respectively. Framework of resolved momentum control is adopted for stepping motion in the latter phase.

Then we showed a sequence of pivoting motion to manipulate the objects towards the desired direction. We have shown that the proposed pivoting manipulation can be effectively realized by computer simulation and experiments using a humanoid robot platform HRP-2.

The method will be improved to adapt to various object shapes of transportation in pursuit of wide application in future developments. Another future extension is the manipulation planning for more general trajectories with experimentation of both manipulation and stepping phases. Integration of identification of objects or environments in contact [15, 16] with the robot is also an important issue to improve the robot's dexterity.

## Acknowledgment

We would like to express our sincere gratitude to Dr. Shuuji Kajita of Humanoid Research Group, Intelligent Systems Research Institute, AIST, for their helpful advice about the control issues. We are also grateful to Prof. Yasumichi Aiyama of Tsukuba University for his references to state of the art in the research field of manipulation.

## References

[1] Y. Aiyama, M. Inaba, and H. Inoue "Pivoting: A new method of graspless manipulation of object by robot fingers," Proc. of the IEEE/RSJ Int. Conf. on Intelligent Robots and Systems, 136 - 143, 1993.

[2] S. Kajita, F. Kanehiro, K. Kaneko, K. Fujiwara, K. Harada, K. Yokoi, and H. Hirukawa. Resolved momentum control: Humanoid motion planning based on the linear and angular momentum, Proc. of IEEE/RSJ Int. Conf. on Intelligent Robots and Systems, 1644-1650, 2003.

[3] M. Mason: “Mechanics and Planning of Manipulator Pushing Operation,” Int. J. Robotics Research, **5**-3, 53-71, 1986.

[4] K. Lynch: “The Mechanics of Fine Manipulation by Pushing,” Proc. IEEE Int. Conf. on Robotics and Automation, 2269-2276, 1992.

[5] A. Bicchi, Y. Chitour, and A. Marigo: “Reachability and steering of rolling polyhedra: a case study in discrete nonholonomy,” IEEE Trans. on Automatic Control, **49**-5, 710-726, 2004.

[6] Y. Maeda and T. Arai: “Automatic Determination of Finger Control Modes for Graspless Manipulation,” Proc. of IEEE/RSJ Int. Conf. on Intelligent Robots and Systems, 2660-2665, 2003.

[7] H. Yoshida, K. Inoue, T. Arai, and Y. Mae: “Mobile manipulation of humanoid robots-optimal posture for generating large force based on statics,” Proc. of IEEE Int. Conf. on Robotics and Automation, 2271 - 2276, 2002.

[8] Y. Hwang, A. Konno and M. Uchiyama: “Whole body cooperative tasks and static stability evaluations for a humanoid robot,” Proc. of IEEE/RSJ Int. Conf. on Intelligent Robots and Systems, 1901 - 1906, 2003.

[9] H. Harada, S. Kajita, F. Kanehiro, K. Fujiwara, K. Kaneko, K. Yokoi, and H. Hirukawa: “Real-Time Planning of Humanoid Robot’s Gait for Force Controlled Manipulation,” Proc. of IEEE Int. Conf. on Robotics and Automation, 616-622, 2004.

[10] T. Takubo, K. Inoue, K. Sakata, Y. Mae, and T. Arai. Mobile Manipulation of Humanoid Robots - Control Method for CoM Position with External Force -, *Proc. of IEEE/RSJ Int. Conf. on Intelligent Robots and Systems*, 1180-1185, 2004.

[11] H. Harada, S. Kajita, H. Saito, M. Morisawa, F. Kanehiro, K. Fujiwara, K. Kaneko, and H. Hirukawa: “A Humanoid robot carrying a heavy object,” Proc. of IEEE Int. Conf. on Robotics and Automation, 1724-1729, 2005.

[12] N. E. Sian, K. Yokoi, S. Kajita, K. Tanie. Whole Body Teleoperation of a Humanoid Robot Integrating Operator's Intention and Robot's Autonomy - An Experimental Verification -, *Proc. of IEEE/RSJ Int. Conf. on Intelligent Robots and Systems*, 1651-1656, 2003.

[13] F. Kanehiro, N. Miyata, S. Kajita, K. Fujiwara, H. Hirukawa, Y. Nakamura, K. Yamane, I. Kohara, Y. Kawamura and Y. Sankai: "Virtual humanoid robot platform to develop ", Proc. of IEEE/RSJ Int. Conf. on Intelligent Robots and Systems, 1093 - 1099, 2001.

[14] K. Kaneko, F. Kanehiro, S. Kajita, H. Hirukawa, T. Kawasaki, M. Hirata, K. Akachi and T. Isozumi: "The Humanoid Robot HRP-2", Proc. of IEEE/RSJ Int. Conf. on Robotics and Automation, 1083-1090, 2004.

[15] Y. Yu, K. Fukuda, and S. Tsujio: "Estimation of Mass and Center of Mass of Graspless and Shape-Unknown Object," Proc. of IEEE Int. Conf. on Robotics and Automation, 2893- 2898, 1999.

[16] T. Debus, P. Dupont and R. Howe: "Automatic Identification of Local Geometric Properties During Teleoperation," Proc. of IEEE International Conference on Robotics and Automation, 3428 - 3434, 2000.